

# Electronic Energy Transfer and Quantum-Coherence in $\pi$ -Conjugated Polymers<sup>†</sup>

Inchan Hwang and Gregory D. Scholes\*

*Department of Chemistry, 80 St. George Street, Institute for Optical Sciences, and Centre for Quantum Information and Quantum Control, University of Toronto, Toronto, Ontario M5S 3H6, Canada*

*Received August 17, 2010. Revised Manuscript Received October 24, 2010*

Electronic energy transfer (EET) has been the subject of intense research because of its significant contribution to the photophysical properties of various material systems. For  $\pi$ -conjugated polymers, it has long been accepted that a classical hopping mechanism is dominant in the energy transfer dynamics because of a weak electronic coupling. However, recent research reveals that conjugated polymers, in fact, can have an electronic coupling strong enough to preserve quantum-coherence. In this review, we summarize the main photophysical features of conjugated polymers. We discuss how electronic excited states evolve on various time scales from femtoseconds to hundreds of picoseconds in terms of exciton relaxation, localization, and electronic energy transfer. The Förster energy transfer model and modifications needed for describing energy transfer in conjugated polymers are described. We discuss how chain conformation and its disorder influence EET and the time scale of the evolution of electronic excited states, and demonstrate how quantum coherence contributes to energy transfer dynamics. Recent research on exciton diffusion in various kinds of polymers is summarized.

## 1. Introduction

Photoexcitation often results in electronic excitation localized on a molecule or on a distinct light-absorbing unit – a chromophore – in a supramolecular structure. The electronic excitation can be transferred to nearby chromophores (usually within a radius of  $\sim 10$  nm) by the process of electronic (or resonance) energy transfer (EET or RET) provided that two key conditions are satisfied.<sup>1</sup> First, there needs to be a small electronic coupling that causes de-excitation of the donor chromophore and a concomitant excitation of the acceptor.<sup>2</sup> In most cases, this is the Coulombic interaction between transition densities,<sup>3</sup> that acts over a long-range and is approximately described by a dipole–dipole ( $1/R^3$ ) coupling between transition dipoles.<sup>4–6</sup> Second, energy must be conserved. This means that the donor fluorescence spectrum must overlap with the acceptor absorption spectrum.<sup>7</sup>

EET is prevalent in a range of material systems, including supramolecular complexes, aromatic polymers, semiconductor colloids, rare-earth doped crystals, and natural proteins – especially those involved in photosynthesis. It also provides an important contribution to the photophysics of conjugated polymers. As will be described in more detail below, structural disorder breaks the perfect one-dimensional  $\pi$ -conjugation of a conjugated polymer and produces a distribution of conformational subunits that

act as effective chromophores. All of these chromophores along a conjugated polymer chain absorb light, but rapid EET funnels that excitation energy to the large chromophores – generally longer  $\pi$ -conjugated units – meaning that fluorescence is observed from a select distribution of chromophores (see Figure 1). The large Stokes shift between absorption and emission maxima that is typical of conjugated polymers is caused largely by the combined effect of vibrational relaxation (mainly torsional relaxation) and electronic energy transfer to lower energy sites along the chain.<sup>8,9</sup> By studying EET, or more generally the evolution of excited states in conjugated polymers, one can learn about conformational disorder and chain aggregation and how they influence the length scales and strength of  $\pi$ -conjugation.

In this short review, we describe energy-transfer processes in  $\pi$ -conjugated polymers. We first summarize the mechanisms and time scales of EET reported in the literature. In the remainder of the paper we will focus on developing a picture of how electronic excited states evolve on various time scales in conjugated polymers.

## 2. Introduction to Electronic Energy Transfer

By the mid-1900s researchers had documented that excitation energy can be transferred from any electronically excited molecule to a nearby ground state molecule by a kind of “inductive resonance”.<sup>10–15</sup> The process is comparable to the way that vibrations of one mechanical oscillator can be transferred to a second oscillator if the

<sup>†</sup> Accepted as part of the “Special Issue on  $\pi$ -Functional Materials”.

\*Corresponding author. E-mail: gscholes@chem.utoronto.ca.

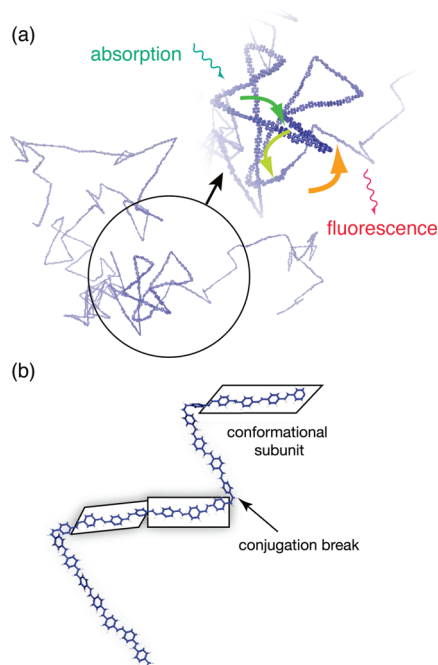


**Figure 1.** (a) Chain conformation of a single polymer chain. The cartoon zoomed in the black circle illustrates the processes of energy transfer between absorption and fluorescence along a chain. (b) Close-up look of a part of a single polymer chain showing conformational subunits produced by conjugation breaks.

oscillators are weakly coupled (e.g., by a weak spring). Excitation is thought of as localized on one molecule, the donor, prior to the transfer event, then it is localized on the acceptor molecule after transfer. It was established that the primary process involved in transferring excitation energy is not a “trivial” mechanism whereby donor fluorescence is reabsorbed by an acceptor, but EET occurs through a quantum mechanical mechanism.<sup>16</sup> Although the result is easily demonstrated by writing the antisymmetrized singlet reactant and product (i.e., before and after energy transfer) configurations of the system, assuming orbital overlap is small and neglecting electron correlation,<sup>17,18</sup> here we are concerned with a qualitative description.

Because of the exponential attenuation of overlap of the donor and acceptor molecular orbitals with distance between molecules, contributions from this kind of interaction (often referred to the Dexter EET) are typically negligible for intermolecular separations of greater than 5 Å, and this is why they are neglected in Förster theory. The primary interaction that promotes energy transfer is thus the quantum mechanical electrodynamic interaction, which is caused by a special two-electron Coulomb integral. Normally we think about such two electron integrals as the repulsion between the charge overlap densities of electron 1 with that of electron 2. There is, however, the Coulombic interaction possible between two transition densities,  $P_{ad}^{\text{donor}}(r_1)$  and  $P_{bb'}^{\text{acceptor}}(r_1)$ .<sup>3</sup> The transition density is a quantum-mechanical concept defined as the off-diagonal density matrix element connecting any two electronic states of a molecule. The quantum-mechanical electrodynamic interaction  $V^{\text{ed}}$  is the long-range

Coulombic coupling between transition densities whereby the de-excitation of the donor molecule resonates with excitation of the acceptor

$$V^{\text{ed}} = 2(ad'|b'b) = \frac{e^2}{4\pi\epsilon_0} \int \frac{P_{ad}^{\text{donor}}(r_1)P_{bb'}^{\text{acceptor}}(r_2)}{|r_1 - r_2|} dr_1 dr_2 \quad (1a)$$

$$\approx \frac{1}{4\pi\epsilon_0} \frac{\kappa\mu_{0L}^A\mu_{K0}^B}{R^3} \quad (1b)$$

When the two molecules A and B are separated by a distance large compared to their size, eq 1a can be represented approximately as a dipole–dipole interaction between electric dipole transition moments, eq 1b, using the usual notation where  $\kappa$  is the orientation factor and  $R$  is the center-to-center intermolecular separation.<sup>2</sup> However, in the case of conjugated polymers, the point-dipole approximation is of limited value, as we discuss below.<sup>19</sup>

The next key ingredient, energy conservation, was obtained from a series of careful experiments, mainly from the groups of Vavilov and Galanin.<sup>10,20,21</sup> It was found that the energy transfer efficiency depends on the overlap of the emission (fluorescence) spectrum of the donor and the absorption spectrum of the acceptor. Förster united these ingredients using the Fermi Golden rule to estimate the energy transfer rate in the limit of very weak electronic coupling between donor and acceptor:<sup>22</sup>

$$k = \frac{2\pi}{\hbar} \int d\epsilon |sV^{\text{ed}}|^2 J(\epsilon) \quad (2)$$

Here,  $s$  is the screening of the electrodynamic interaction  $V^{\text{ed}}$ , assumed in Förster theory to be  $1/n^2$ , where  $n$  is the refractive index of the medium (e.g., solvent). The screening is actually a function of the size, shape, and separation of the chromophores in the medium, and it has been found to confer an additional distance dependence to the energy transfer rate.<sup>23</sup>  $J(\epsilon)$  is the overlap between area normalized spectra; it is not the Förster spectral overlap. The magnitude of the integrated overlap depends not only on the resonance of the two transitions, but also on the spectral line broadening.

The genius of Förster theory is that it connects eq 2 to spectra that can be recorded by the experimentalist. These expressions are well-known and the reader is referred to the literature for further explanation.<sup>2,4,24–26</sup> The Förster critical transfer distance  $R_0$  has proved particularly useful. It is defined as the interchromophore distance  $R$  at which the energy transfer efficiency is 50%. Its application, however, relies on the validity of the point-dipole approximation for the electronic coupling so that the energy transfer efficiency  $E$  is given by eq 3

$$E = \frac{1}{1 + (R/R_0)^6} \quad (3)$$

### 3. Trends in Energy Transfer in Conjugated Polymers

Polarization anisotropy experiments using pump–probe techniques provide information about the dynamics of energy transfer. The polarization anisotropy is defined as<sup>27,28</sup>

$$r(t) = \frac{I_{VV}(t) - I_{VH}(t)}{I_{VV}(t) + 2I_{VH}(t)} \quad (5)$$

The intensities  $I_{VV}$ , measured with a vertically polarized pump pulse and vertically polarized probe pulse, and  $I_{VH}$ , measured with a vertically polarized pump pulse and horizontally polarized probe pulse, are proportional to an induced third-order polarization averaged over the molecular orientations with respect to the pump–probe polarization  $\langle P^{(3)}(0, t_p, t) \rangle$ . The rotational averaging relates the laboratory frame pump and probe pulse polarizations to the dipole transition moments of the molecules being photoexcited.<sup>28–33</sup> For randomly oriented molecules this relationship is governed by an isotropic Cartesian tensor.<sup>34,35</sup> In the anisotropy expression the signal amplitudes can cancel (ideally) except for the factor that gives the time dependence of the ensemble averaged transition dipole randomization,

$$r(t) = \left( \frac{\frac{1}{5} - \frac{1}{15}}{\frac{1}{5} + \frac{1}{15}} \right) \langle P_2(\hat{\mu}(0) \cdot \hat{\mu}(t)) \rangle \quad (6)$$

The prefactor is equal to 0.4 and the latter factor represents the projection of the transition dipole unit vector rotational correlation function, where  $P_2(x)$  is the second-order Legendre polynomial.

The depolarization of emission on ultrafast time scales is caused by excitons migrating along polymer chains<sup>36</sup> or between chains.<sup>37,38</sup> The initial anisotropy is theoretically 0.4. However, possibly due to exciton dynamics that occurs within the laser pulse duration, it is often observed for conjugated polymers that the initial anisotropy is below 0.4.<sup>39–42</sup> The initially low anisotropy suggests that excitation might be depolarized by dynamic conformational disorder,<sup>43</sup> structural relaxation,<sup>41</sup> exciton localization,<sup>38</sup> or possibly fast coherent transfer.<sup>44–46</sup>

It should be noted that the original Förster transfer should be used only if the point-dipole approximation holds. Usually, that is the case when the spatial extent of transition dipoles is much smaller than the distance between the centers of the molecules. In conjugated polymers and oligomers, the point-dipole approximation often fails. For example, Beljonne, et al. examined electronic couplings between indenofluorene oligomers.<sup>47</sup> Results obtained from quantum chemical methods were compared to electronic couplings obtained within a simple point–dipole model. Although the point-dipole model correctly reproduced the qualitative evolution of electronic couplings with donor–acceptor separation, for linear chromophores, it considerably underestimated (by about 1 order of magnitude) the electronic couplings and transfer rates in

comparison to the description provided on the basis of the atomic transition densities. It was concluded that the point–dipole model cannot adequately account for the spatial distribution of the excitations over nearby donor and acceptor oligomers and that this is a particularly significant issue for linear chromophores. Rossky and co-workers examined the interactions between two  $\pi$ -conjugated molecules.<sup>48</sup> They found that generally the energy transfer rate shows a significantly weaker short-range distance dependence than anticipated (closer to  $R^{-2}$  than to  $R^{-6}$ ) and the Förster expression overestimates the energy transfer rate by more than 2 orders of magnitude at short separation. It was also found that significant excitation transfer can occur via states that are optically dark. They conclude that the Förster expression is inappropriate for condensed-phase systems where donors and acceptors can be closely packed, as, for example, in thin films. That was also concluded by Walla et al. in a study of electronic couplings between carotenoids.<sup>49</sup>

There have been many approaches to improve the original Förster transfer. Krueger et al. realized that the multipole expansion methods were of limited value and that the most direct approach was to calculate transition densities for the donor and acceptor directly using quantum-chemical methods, then compute the coupling between them.<sup>3</sup> This method, known as the transition density cube (TDC) approach, has proven to be accurate and versatile. Less computationally demanding methods include the extended dipole model (or the line-dipole model)<sup>39,48,50–52</sup> and the multicentric monopole expansion model.<sup>19,44,49,53,54</sup> All the improved models suggest that the point-dipole approximation under- and overestimates the electrodynamic coupling for head-to-head and cofacial transition dipole configurations, respectively. For intrachain energy transfer, for example, calculation of electronic coupling using quantum chemical methods that avoid the point-dipole approximation reveals the electronic coupling decreases markedly with the increasing size of the donor and the acceptor.<sup>44</sup> This can be attributed to the fact that the transition density amplitude at the edges of donor and acceptor decreases as the chromophore size increases.

Consistent with theoretical studies, it has been observed that energy transfer in films is a few orders of magnitude more efficient than the energy transfer in solution.<sup>47</sup> This suggests that interchain energy transfer is faster than intrachain energy transfer. That is in part due to the closer separation that can be attained between cofacially packed chromophores, but is also caused by a breakdown of the point-dipole approximation.<sup>47,49</sup> Similarly, Nguyen et al. observed faster interchain energy transfer in MEH-PPV than intrachain EET by partly constraining the MEH-PPV chains in an ordered mesoporous silica matrix.<sup>55,56</sup> In the regime where interchain energy transfer is significant, the point-dipole approximation breaks down. Therefore, in order to analyze energy transfer quantitatively, particularly in films, it is necessary to modify the original Förster transfer.

When the Förster energy transfer model breaks down, a generalized Förster critical distance  $R_G$  for the donor–acceptor pair has been proposed.<sup>57</sup> The ratio of the more precisely determined electronic coupling,  $V$ , to that estimated using the dipole–dipole formula (see eq 1b),  $V^{dd}$ , enables a scaling factor  $\eta = (V/V^{dd})^{1/3}$  to be found so that

$$R_G = \eta R_0 \quad (4)$$

$R_G$  can then be substituted for  $R_0$  in eq 3.

The time scales of exciton localization and inter- and intrachain EET are summarized in Table 1. Details of exciton localization will be discussed later. Notably, each process has distinctively different time scales, ranging from femtoseconds to subnanoseconds. Most of the energy migration that ultimately produces the population of conformational subunits from which fluorescence originates happens during time scales of  $\sim 1$ –10 ps. The inhomogeneity in time scales reflects that hierarchy of structural characteristics of conjugated polymers, as we discuss in the following section of this review.

The photophysical properties contributed by EET depend significantly on the chain conformation such as the size of a chain and the distribution of distances between conformational units. These factors have been probed by single molecule spectroscopy studies of MEH-PPV.<sup>58–61</sup> If a chain has a self-collapsed conformation, then the distance between segments is short enough that excitation energy can efficiently be funneled to a single conjugated segment, because all segments are effectively within the Förster radius. On the other hand, if a chain is more or less stretched, forming an open conformation, EET is inefficient. Schindler and co-workers observed zero-phonon lines in fluorescence with a spectral width of a few meV for MEH-PPV and MeLPPP dispersed in

a polystyrene matrix at 5 K.<sup>62</sup> This observation indicates one single chromophore only undergoes fluorescence, while the rest of chromophores do not contribute to fluorescence. This conclusion is supported by Lin and co-workers through single molecule studies on MEH-PPV. They suggested that the entire polymer chain does not take part in the generation of emissive excitons, especially for self-collapsed chains.<sup>63</sup> Nonemissive sites are thought to be mostly in aggregated regions of a polymer chain. Even if the photogenerated excitons are bright states (therefore potentially emissive), they cannot contribute to the steady-state fluorescence spectrum once excitation is transferred to nonemissive, dark, sites by EET.

One might now consider a multistep energy-transfer process, which is called exciton migration.<sup>64</sup> From anisotropy decay experiments, energy transfer in conjugated polymers in solution and films has been found to occur on a picosecond or longer time scale,<sup>39,41</sup> which is much slower than relaxation and decoherence times. Exciton localization occurs in tens of femtoseconds because of coupling to the torsional modes.<sup>37,42</sup> Therefore, although coherent energy transfer has been observed in MEH-PPV chloroform solution,<sup>45,46</sup> in many cases exciton migration occurs, on average, by incoherent dynamics (such as in the Förster energy-transfer model). This is typically labeled exciton diffusion.

The exciton diffusion length in films varies among kinds of conjugated polymers, but has been found to be approximately 10 nm (see Table 2) determined by various kinds of studies; photoconductivity action spectra<sup>65–67</sup> and stationary/time-resolved luminescence quenching studies.<sup>68–77</sup> One can determine the diffusion length from the fit of photocurrent or internal quantum efficiency spectrum of a device with numerical models such as exciton diffusion and discrete hopping models.<sup>65–67</sup> In the study of stationary fluorescence quenching, the diffusion length is determined by fitting the ratio between unquenched and quenched fluorescence at the probe wavelength using a relation developed from the diffusion equation. On the other hand, the diffusion length can be determined also by multiplying the diffusion constant by the exciton lifetime. The diffusion constant is determined by the fit to the time-resolved fluorescence quenched by the interfaces, using a diffusion equation. The exciton lifetime can be measured by time-correlated single photon

**Table 1. Comparison of Time Scales and Effects of Exciton Localization and Inter/Intrachain EET on Polarization Anisotropy**

process	EET time scale	effects on anisotropy
exciton localization	$\sim 100$ fs	initial anisotropy is smaller than 0.4
interchain EET	ps to tens of ps	depolarization with population time
intrachain EET	tens of ps to hundreds of ps	

**Table 2. Exciton Diffusion Length in Conjugated Polymers<sup>a</sup>**

polymer	method/quencher	diffusion length (nm)	ref
P3HT	steady-state PLQ/TiO <sub>2</sub>	$7.5 \pm 1$	69
P3HT	time-resolved PLQ/TiO <sub>2</sub>	$8.5 \pm 0.7$	70
P3HT	steady-state PLQ/pyrolytic graphite	$7 \pm 1$	71
PPV	short-circuit photocurrent fit/ $C_{60}$	$7 \pm 1$	66
NRS-PPV		$5 \pm 1$	
BEH-PPV	time-resolved and steady-state PLQ/ $C_{60}$	$6 \pm 1$	76, 77
MEH-PPV		$6.3 \pm 1$	
MDMO-PPV	steady-state PLQ/TiO <sub>2</sub>	$6 \pm 1$	78
F8BT	steady-state PLQ and ELQ/Ca	$\sim 5$	73
F8BT	Steady state PLQ/PEDT:PSS	10–15	74
LPPP (ladder-type poly( <i>p</i> -phenylene))	steady-state PLQ & time-resolved stimulated emission quenching/ $C_{60}$	14	75

<sup>a</sup> PLQ and ELQ stand for photoluminescence quenching and electroluminescence quenching, respectively.



counting measurements. For accurate determination of the exciton diffusion length using fluorescence quenching techniques, two concerns are the effects of optical interference and of energy transfer from the polymer film to the quencher film on luminescence quenching. It has been suggested that these problems can be resolved by using a thin  $\text{TiO}_2$  film with less than 5 nm thickness.<sup>78</sup> In addition, it should be noted that the exciton diffusion length determined by luminescence quenching studies is the diffusion length only perpendicular to the substrate. Because in many cases conjugated polymers are preferentially lying in an in-plane orientation relative to the substrate,<sup>79,80</sup> the in-plane diffusion length is expected to be different.

The diffusion coefficient of excitons is often assumed time-independent for simplicity. However, in the presence of energetic and orientational disorder, the diffusion coefficient should be considered to be time-dependent.<sup>81–83</sup> Indeed, for conjugated polymers, the time-dependence of the exciton diffusion coefficient has been considered to explain exciton transport, because they migrate in a Gaussian density of states, which is broadened due to energetic disorder.<sup>65,72,84–88</sup> Excitons diffuse quickly at early times, but more slowly with time. The origin of a decrease in the diffusion coefficient with time can be explained by the relaxation of excitons to the lower energy sites which have lower exciton hopping probabilities; in conjugated polymers, high energy excitons, on shorter subunits, can be transferred downhill to any other subunits in a Gaussian density of states, but as excitons reach lower energy subunits, the number of suitable acceptors within the Förster radius diminishes.<sup>89–91</sup> Another origin of the time-dependent diffusion coefficient is traps such as aggregates. The rate of transfer from aggregates is often considered to be negligible or very small compared to the transfer rate between nontrap sites and toward the traps.<sup>92</sup> Athanasopoulos et al. found that the dynamics of exciton transport are not affected by the presence of traps at short times (< 10 ps), but are slowed down at longer times, because of the fact that excitons transfer to the nontrap sites with high probability at short times but they are captured by the traps with time.<sup>93</sup>

The exciton diffusion length is one of the key parameters in determining efficiency of polymer based diodes. For light-emitting diodes, a small diffusion length is preferred to prevent exciton quenching, for example, dissociation at the metal electrode interface, defects or heterojunction interfaces before radiative recombination. In contrast, for photovoltaic devices, a long diffusion length of excitons is desirable in order for excitons to reach the interface (e.g., with PCBM) in bilayer heterostructures or polymer blends with large domain sizes. A popular way to overcome the problem of the short exciton diffusion length is to control film morphology.<sup>94</sup> However, it was found that fine morphology might not be optimal for power conversion efficiency, as it causes inefficient dissociation of polaron pairs. Coarse morphology is rather better in order for charges to escape from their counterpart charges once excitons reach heterojunction interfaces.<sup>95</sup> Therefore, one

of the best solutions to efficient photovoltaic devices with respect to exciton diffusion and polaron-pair dissociation is to have coarse morphology and long exciton diffusion lengths. Scully and co-workers show that the large Förster radius enhanced by the large spectral overlap between the donor with a high quantum yield and the acceptor with a high absorption coefficient increases an exciton diffusion length, but power conversion efficiency still needs to be improved.<sup>96</sup>

#### 4. Conformational Subunits and Conjugated Polymer Excited States

In this section, we consider the chromophores of conjugated polymers in more detail. A perfect conjugated polymer would have  $\pi$ -orbitals delocalized in one dimension along the chain and its electronic structure would therefore be described well by the semiconductor band model. Schott and co-workers have reported close to ideal polydiacetylene chains with extraordinary coherence lengths.<sup>97,98</sup> However, it is generally found that conjugated polymer chains are highly disordered and therefore twists of the chain break the  $\pi$ -conjugation into basic chromophores, called conformational subunits, as illustrated in Figure 1. Nevertheless, a chain of noninteracting conformational subunits is not quite the correct description of a conjugated polymer. In fact, conformational subunits can interact, forming delocalized collective states, as we will discuss in this section. There are two ways of thinking about the manifestation and consequences of conformational disorder.

There are many twists and kinks along the polymer backbone leading to an inhomogeneous distribution of chromophores – spanning from about two to ten polymer repeat units. One of the significant consequences of this conformational disorder is inhomogeneous broadening. Inhomogeneous broadening arises from a distribution of sizes (and thus energies) of chromophores that comprise a conjugated polymer chain. Inhomogeneous broadening can be investigated also by site-selective fluorescence<sup>99–101</sup> and spectral hole-burning studies.<sup>102–104</sup> Both techniques are used to eliminate inhomogeneous broadening by photoselection of a narrow distribution of chromophores, thus revealing the homogeneous line broadening of electronic transitions. A consequence of inhomogeneous broadening in conjugated polymer is that excitation on the blue edge of the absorption spectrum mainly excites short subunits, and energy transfer causes that excitation energy to migrate “downhill” to longer, more red-absorbing, conformational subunits. In other words, excitation energy above a certain threshold energy leads to emission independent of the excitation energy, indicating that excitation energy is funneled to a common lowest lying excited state regardless of the initial excitation energy, which has been revealed by Bäessler and co-workers and other groups.<sup>99,100,105–107</sup> This conclusion is in agreement with single molecule studies.<sup>108</sup> It has been found that spectral overlap is favorable and electronic coupling is caused by the Coulombic interaction between the chromophores.<sup>47</sup> This model is well-suited to describe

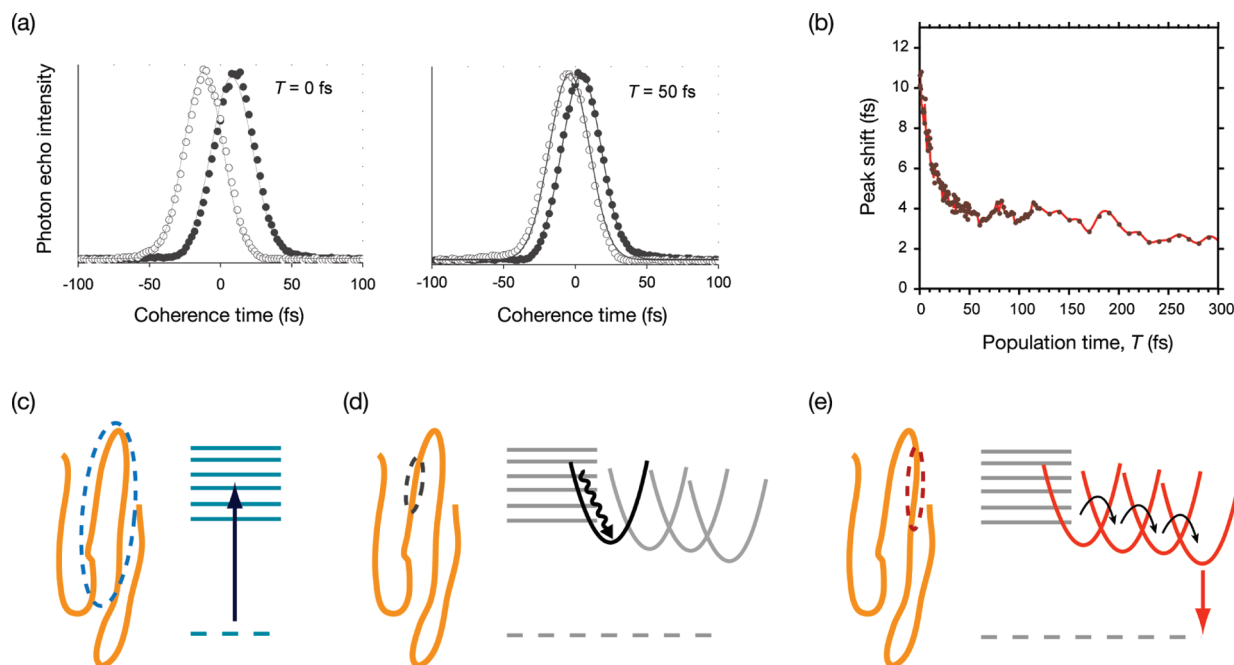


**Figure 2.** (a) Three-pulse photon echo signals versus coherence time for population times  $T = 0$  and 50 fs for a dilute MEH-PPV solution in chlorobenzene. The signal peaked at positive coherence times is the rephasing signal (closed circles), and peaked at negative coherence times is the nonrephasing signal (open circles). (b) The peak shift as a function of population time. The evolution of excited states is illustrated in chronological order: (c) Delocalization of an exciton created by photoexcitation, (d) exciton localization, and (e) electronic energy transfer in a single polymer chain are illustrated and their schematic of electronic structures and potential energy surfaces for each event are schematically illustrated. Panels a and b are adapted with permission from ref 111. Copyright 2005 American Physical Society.

the picosecond and longer dynamics of EET along and between conjugated chains.<sup>39,44</sup>

This static picture of weakly interacting chromophore subunits, however, is not ideally suited for understanding a number of other experiments. For example, electron transport measurements of single conjugated oligomers show that coherent charge transport (tunneling) dominates up to a certain length, then activated hopping becomes important as conformational disorder breaks the coherence.<sup>109</sup> A question is how we can best describe the transition from tunneling to hopping. Similar questions arise for ultrafast EET. In this respect, photon echo spectroscopy has been revealing.

In photon echo experiments, the first pulse produces a superposition of excitations in the ensemble, each with a different natural frequency owing to inhomogeneous line broadening. The final pulse in the sequence induces “rephasing”. That is, the inhomogeneous dephasing, which appears in the first period between the first and the second pulses, is canceled by the action of the third pulse, and thus a signal so-called the photon echo is generated. In many cases this experiment allows us to detect properties that are usually obscured by inhomogeneous line broadening.

One of the examples of photon echo experiments is the three-pulse photon echo peak shift (3PEPS).<sup>110,111</sup> Figure 2a shows the peak shift of the time-integrated photon echo signal on the coherence time axis for MEH-PPV in solution. This represents the rephasing capability of the ensemble after a certain population time  $T$ . A reduction in the peak shift with the population time as shown in Figure 2b is caused by spectral diffusion and indicates loss of memory of

the initial electronic transition frequency distribution due to, for example, stochastic interaction with the local environment. The nonzero asymptotic peak shift after long population times observed for MEH-PPV in solution suggests that the inhomogeneous line width is comparable to the homogeneous line width. Interpretation of the 3PEPS of MEH-PPV solution required starting from a model when electronic excitation is somewhat delocalized. For example, the photogenerated excitons could be modeled by employing the Su-Schrieffer-Heeger (SSH) Hamiltonian including disorder in the transfer matrix elements between repeat units.<sup>112,113</sup> Therefore, excitons formed by photoexcitation are initially delocalized across multiple chromophores on a single chain<sup>114,115</sup> or in packed chains (Figure 2c).<sup>116,117</sup> The initial dynamics that decay the 3PEPS are then assigned to relaxation among these exciton states together with dynamic localization caused by decoherence (Figure 2d). After approximately 100–200 fs the excitation is localized more-or-less to a conformational subunit and energy transfer proceeds on longer time scales by a hopping (Förster) mechanism (Figure 2e). Although this energy migration is thought to be mainly a hopping processes from excitation localized on a conformational subunit, the acceptor excited states are delocalized—just like the initially photoexcited states.<sup>118</sup> Hence energy transfer should be more correctly modeled by using Generalized Förster Theory<sup>44</sup> or the method employed by Singh and co-workers.<sup>119</sup>

The model suggested by 3PEPS is supported by ultrafast anisotropy experiments. When a system of randomly oriented polymer chains interacts with polarized light, the probability that any chromophore in the ensemble will

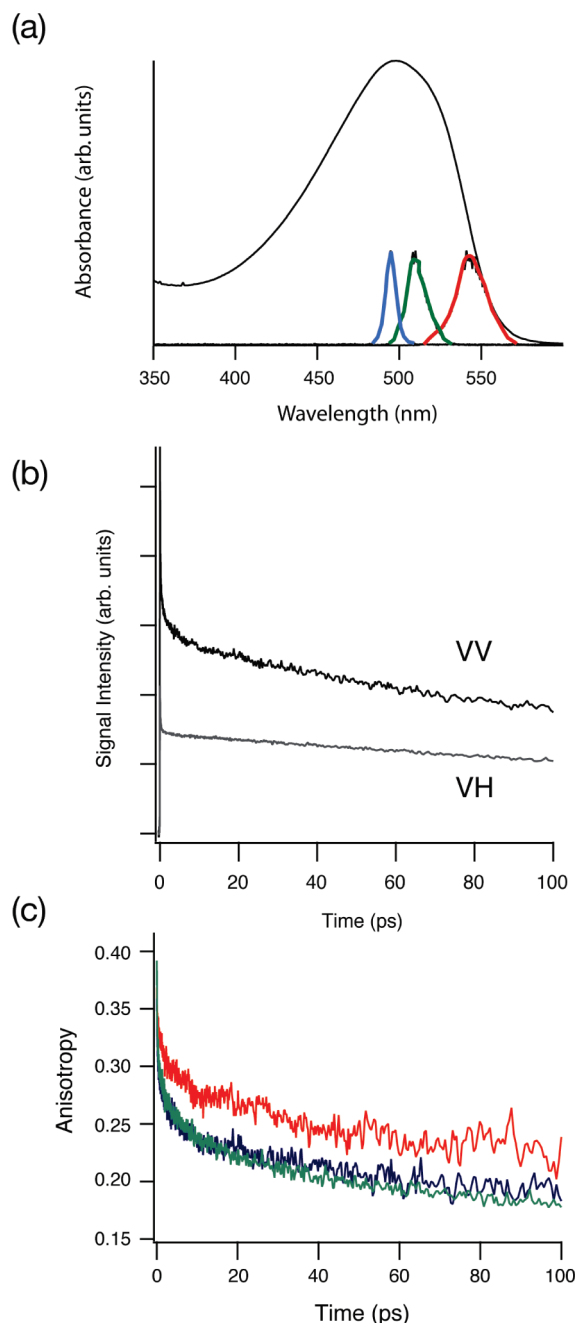


**Figure 3.** (a) Absorbance for MEH-PPV in chlorobenzene solution and normalized laser spectra with center wavelength of 493 nm (blue), 510 nm (green), and 540 nm (red). (b) The intensities  $I_{VV}$  and  $I_{VH}$  as a function of population time at an excitation of 493 nm. (c) Pump-probe anisotropy versus population time at 493 nm (blue), 510 nm (green), 540 nm (red) the pump-probe wavelengths. Adapted and modified with permission from ref 120. Copyright 2009 American Chemical Society.

absorb light depends upon the projection of its transition moment with respect to the polarization of the electric field vector of the incident light. That is, when the sample is excited by polarized light, the transition dipole needs to be oriented (at least partly) in the direction of polarization. This is the initially prepared state; from this distribution of states, relaxation will occur. If that relaxation involves a change in the orientation of transition dipoles, then a concomitant change of anisotropy is observed in the ensemble measurement.<sup>28,32</sup>

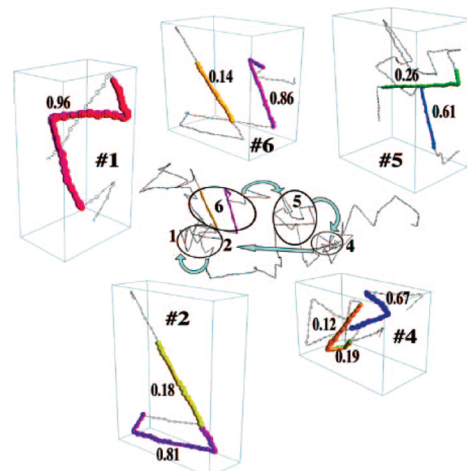


**Figure 4.** Delocalization of electronic eigenstates in the dressed eigenstate representation at the primary excitation moves along a polymer chain. The cartoon in the center represents exciton relaxation between eigenstates. The coloration denotes the net amplitude of an excited eigenstate. Less than 10% of amplitude is not shown. For example, for state 1, the color coding indicates that 96% of amplitude is delocalized over one large conformational subunit and the remaining 4% of amplitude is delocalized over the rest of segments, which is not shown. For state 4, the color coding denotes that 67, 19, and 12% of the amplitude are delocalized over the three different conformational units. Adapted with permission from ref 119. Copyright 2009 American Institute of Physics.

Typical  $I_{VV}$  and  $I_{VH}$  pump-probe traces for MEH-PPV in solution are plotted in Figure 3 (b). Figure 3 (c) demonstrates the excitation wavelength dependence of the anisotropy decay of MEH-PPV in chlorobenzene as measured by one-color pump-probe. Excitation wavelengths were 493, 510, and 540 nm. The anisotropy decays rapidly during the first  $\sim 200$  fs, after which it assumes a significantly slower decay profile that ultimately accounts for most of the anisotropy decay. These decay processes are attributed to exciton relaxation and energy transfer respectively.

Modeling of these pump-probe experiments suggested that the ultrafast components of the anisotropy decay cannot be understood by the Förster EET model. It was found that population relaxation among states delocalized over more than a single conformational subunit, as proposed from analysis of the 3PEPS measurements, was likely to precede energy transfer hopping from one chromophore to another. In subsequent work, the nature of the delocalized states and their relaxation dynamics were further elucidated (see Figure 4).<sup>119</sup>

The ultrafast contribution to energy transfer dynamics is highly complicated. From the preceding discussion it is already clear that population relaxes among delocalized electronic states while those same states localize (decohere). A good description for ultrafast EET dynamics in conjugated polymers is as follows. Relaxation among delocalized states is mediated by coupling between electronic states and the bath (random fluctuation of the environmental polarization). However, because excitation is sparsely delocalized (cf. Figure 4), relaxation involves excitation jumping through space. That is promoted by electronic coupling (like in the Förster theory). This picture for population dynamics is suggested by 3PEPS and ultrafast

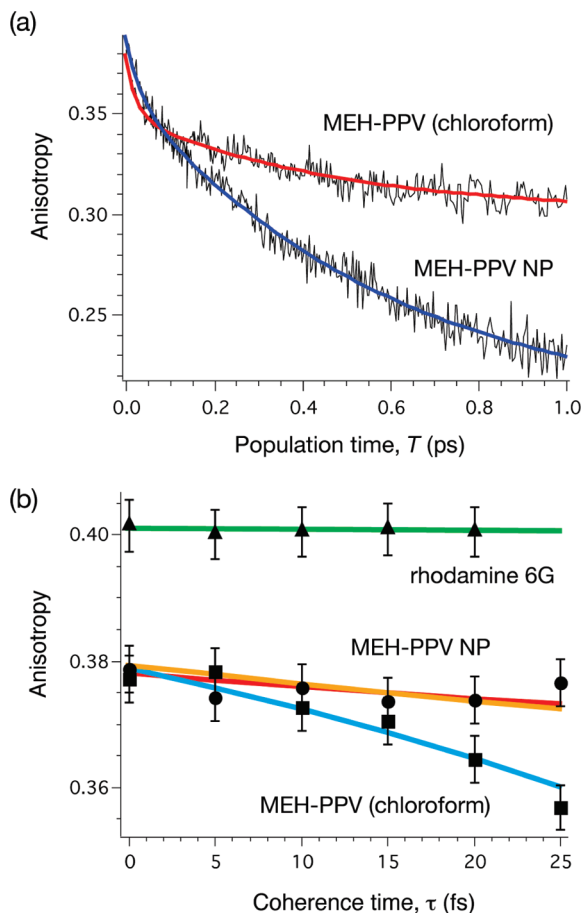


**Figure 5.** Two-time anisotropy decay as a function of (a) population time at  $\tau = 0$  and (b) coherence time at  $T = 0$  for a solution of MEH-PPV in chloroform (red curve in a and squares in b) and aqueous suspension of MEH-PPV NPs (blue curve in a and circles in b). The green solid line in b is a linear fit of the experimental points for Rhodamine 6G (triangles). The orange, red, and cyan solid curves in b represent the simulation results. The anisotropy versus coherence time for Rhodamine 6G in ethanol is shown for reference. No decay in the anisotropy for Rhodamine 6G indicates that the artifacts affecting anisotropy along  $\tau$  axis are sufficiently minimized. Adapted with permission from ref 46. Copyright 2009 Science.

pump–probe anisotropy experiments.<sup>110,111,120</sup> These dynamics are evident in the anisotropy decays, Figure 5(a), where MEH-PPV in solution is compared to collapsed chains in MEH-PPV nanoparticles. The faster EET evident in the nanoparticles is due to efficient interchain EET.

On these ultrafast time scales, we should ask whether quantum-coherent dynamics are also involved. Therefore, recently we probed whether the electronic excitation evolves solely according to population dynamics, and therefore follows classical probability laws, or whether quantum-coherent evolution contributes on ultrafast time scales. To answer this question, we designed a variation of the pump–probe anisotropy experiment called two-time anisotropy decay (TTAD).<sup>45,46</sup> This experiment measures whether an electronic coherence undergoes energy transfer in competition with subsequent population transfer. The results, Figure 5b, indicate that quantum-coherent dynamics occur, but primarily for intrachain EET rather than for interchain energy transfer. This suggests that the polymer's structure supports (low-frequency) phonons with long length scales compared to the exciton size,<sup>121</sup> leading

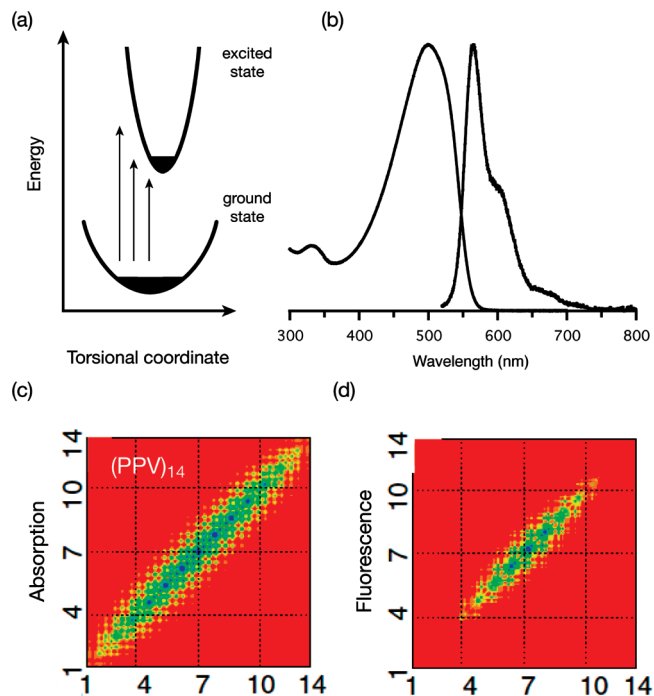


**Figure 6.** (a) Schematic of torsional vibration potentials in the ground and excited states for conjugated polymers. The black shading illustrates the thermal population of each potential, reflecting the origin of a broader spread of energies in absorption than emission. (b) Absorption and emission spectra for MEH-PPV solution in chlorobenzene at room temperature. (c, d) Contour plots of transition density matrices for 14 PPV oligomers. (c) Transition from the ground state (equilibrium geometry) to the lowest excited state. (d) Transition from the excited state (equilibrium geometry) to the ground state. Panels a and b are adapted and modified with permission from ref 141. Copyright 2008 World Scientific Publishing. Panels c and d are adapted with permission from ref 114. Copyright 2002 American Physical Society.

to correlated bath fluctuations and effectively reduced decoherence along a chain.<sup>122</sup>

We conclude by noting that the delocalization issue is important not only for excitons, but also for polarons. Recent numerical calculations of polaron-pair dissociation yield in polymer:fullerene blends suggest that delocalization of charge carriers in a chromophore significantly affects the local mobility of charge carriers.<sup>123</sup> The more delocalized the polaron pairs, the higher local mobility for charge carriers and the higher probability of polaron-pair dissociation.

## 5. Role of Torsional Modes

Nonmirror image absorption–emission spectra of conjugated polymers are often observed at ambient temperature, as the example for MEH-PPV shows in Figure 6b; the absorption is spectrally broad and unstructured, and the emission is narrow and has clear vibronic features. The origin of these different lineshapes has been explained by a combination of conjugated polymer photo-physics and the effect of energy migration. We have already explained how conformational subunits are excited with a broad energy distribution owing to conformational disorder, and subsequently electronic excitation is transferred mostly to the lowest energy chromophores, which often correspond to the longest conformational



units or sometimes interchain species. Therefore, the distribution of emission energies is narrow compared to that of absorption energies.

The fact that conjugated oligomers exhibit a similar shape in their absorption spectra compared to conjugated polymers suggests that the broad and unstructured absorption spectrum is not caused solely by conformational disorder in polymer chains—and in fact it is intrinsic to the chromophore.<sup>124,125</sup> Karabunarliev and co-workers have shown using semiempirical quantum chemical calculations that low-energy torsional modes become stiffer in the excited state than the ground state.<sup>126,127</sup> Similarly, theoretical studies employing *ab initio* quantum chemical calculations for oligomers and polymers have shown that the potential as a function of torsion angle in the excited state is steeper than the ground state.<sup>128–133</sup> Torsional potentials in the ground and excited states are illustrated schematically in Figure 6a. In some cases, torsions change frequency between the ground and excited state having a potential energy minimum at the same torsion angle, 0°. <sup>132,134</sup> However, in general, it is widely accepted that conjugated polymers in the ground state are twisted, whereas they tend to form a planar conformation in the excited state.<sup>130,135,136</sup> The thermal population of torsion angles on the ground state leads to a distinctly nonequilibrium distribution when projected onto the steeper excited state potential by photoexcitation. Torsional relaxation prior to fluorescence results in the narrow emission spectrum. Absorption, on the other hand, occurs with a broad distribution of transition energies, leading to a broad and unstructured spectrum.

In conjugated polymers, it is speculated that the torsional modes play an important role in exciton localization. The torsional modes couple to excitons delocalized over multiple chromophores (Figure 2c), and consequently excitons become localized to the center of conjugated chromophores (Figure 2d).<sup>114,137,138</sup> The center corresponds to where the bond length alternation is minimized in the excited state. Theoretical studies revealed that for PPV, excitons are delocalized upon photoexcitation, but become localized over ~6 repeat units at equilibrium, as shown in panels c and d in Figure 6. One should note that the exciton localization is attributed to the fact that the electronic coupling between transition dipoles on interacting chromophores is weaker than the exciton–phonon coupling.<sup>37</sup> It is also worth mentioning that exciton localization is a consequence of the dynamic coupling between nuclear and electronic degrees of freedom rather than static coupling, causing dephasing of the ensemble coherence.<sup>115,139</sup>

## 6. Conclusions

We have reviewed theoretical and experimental aspects of electronic energy transfer in conjugated polymers. The Förster energy-transfer model is often used to describe the transfer of excitation energy between conformational subunits along conjugated polymer chains, assuming a weak electronic coupling between those subunits compared

to the coupling with the bath of nuclear degrees of freedom. One problem with this model is that the point-dipole approximation assumed in the Förster energy-transfer model is inappropriate to quantitatively analyze energy transfer observed in conjugated polymers. Various procedures for calculating the electronic coupling in conjugated polymers more accurately have been suggested and successfully describe the nature of energy transfer. Examples include the line-dipole model, the multicentric monopole expansion model, and the transition density cube model. Certain studies such as polarization anisotropy, photon echo experiments, and numerical calculations have revealed that exciton delocalization and localization affect the mechanism of ultrafast energy transfer. Indeed, even for a hopping mechanism, excitation energies are transferred from localized to delocalized states in the manner described by generalized Förster theory. Moreover, it was recently found that quantum-coherence is involved in the ultrafast energy-transfer process along a polymer chain, that is, excitation energy is transferred coherently between slightly delocalized states along a chain. Hence the dynamical evolution of excitations in conjugated polymers can be considerably more complicated than previously thought.

A general qualitative conclusion is that excitons migrate quickly (high exciton diffusion constant) at early times, and then more slowly between more localized states at later times after photoexcitation. Energetically downhill energy transfer occurs within a Gaussian density of states and the transfer to aggregates are often seen in films. These kinetics collectively give rise to a short exciton diffusion length of ~10 nm, typically found in conjugated polymers. This is one of the biggest concerns among researchers because it is a factor limiting the efficiency of polymer photovoltaic devices. Many groups are working at resolving this problem by altering film morphologies. Quantum coherent energy transfer has been observed in conjugated polymers, but can it help increase exciton diffusion length if optimized? A theoretical study employing a modified Redfield equation for the exciton density matrix showed that quantum-coherence helps excitons move farther than it would if only incoherent energy transfer processes are considered.<sup>140</sup> This issue still remains open at the present. It may turn out that the solution lies not only in increasing exciton diffusion length in pristine conjugated polymer domains, but also in optimizing long-range energy transfer to the interface with the electron acceptor, thereby bypassing the diffusion bottleneck.

**Acknowledgment.** The Natural Sciences and Engineering Research Council of Canada is gratefully acknowledged for support of this research.

## References

- (1) Förster, T. *Discuss. Faraday Soc.* **1959**, 27, 7.
- (2) Scholes, G. D. *Annu. Rev. Phys. Chem.* **2003**, 54, 57.
- (3) Krueger, B. P.; Scholes, G. D.; Fleming, G. R. *J. Phys. Chem. B* **1998**, 102, 5378.
- (4) Andrews, D. L. *J. Nanophotonics* **2008**, 2, 022502.
- (5) Andrews, D. L. *Chem. Phys.* **1989**, 135, 195.
- (6) Andrews, D. L.; Bradshaw, D. S. *Eur. J. Phys.* **2004**, 25, 845.

- (7) Förster, T. *Ann. Phys.* **1948**, 2, 55.
- (8) Rauscher, U.; Schütz, L.; Greiner, A.; Bässler, H. *J. Phys. Condens. Matter* **1989**, 1, 9751.
- (9) Grozema, F. C.; Siebbeles, L. D. A.; Gelincik, G. H.; Warman, J. M. *Top. Curr. Chem.* **2005**, 257, 135.
- (10) Vavilov, V. I.; Galanin, M. D. *Dokl. Akad. Nauk USSR* **1949**, 67, 811.
- (11) Vavilov, S. I. *Izv. AS USSR Phys.* **1945**, 9, 283.
- (12) Vavilov, S. I. *Dokl. Akad. Nauk USSR* **1950**, 73, 1145.
- (13) Oginets, V. T. *Izv. Vyssh. Uchebn. Zaved. Fiz.* **1976**, 4, 128.
- (14) Sveshnikova, E. B.; Ermolaev, V. L. *Izv. Akad. Nauk SSSR Ser. Fiz.* **1971**, 35, 1481.
- (15) Galanin, M. D. *Akad. Nauk SSSR* **1960**, 12, 3.
- (16) Kallmann, H.; London, F. Z. *Phys. Chem.* **1929**, 2, 207.
- (17) Scholes, G. D.; Ghiggino, K. P. *J. Phys. Chem.* **1994**, 98, 4580.
- (18) Olaya-Castro, A.; Scholes, G. D. *Int. Rev. Phys. Chem.* **2011**, accepted.
- (19) Wisenhofer, H.; Beljonne, D.; Scholes, G. D.; Hennebicq, E.; Brédas, J.-L.; Zojer, E. *Adv. Funct. Mater.* **2005**, 15, 155.
- (20) Galanin, M. D. *Ekspl. Teoret. Fiz.* **1955**, 28, 485.
- (21) Galanin, M. D. *Akad. Nauk S.S.S.R.* **1960**, 12, 3.
- (22) Knox, R. S. *Physica* **1968**, 39, 361.
- (23) Scholes, G. D.; Curutchet, C.; Mennucci, B.; Cammi, R.; Tomasi, J. *J. Phys. Chem. B* **2007**, 111, 6978.
- (24) Agranovich, V. M.; Galanin, M. D. *Electronic Excitation Transfer in Condensed Matter*; North-Holland: Amsterdam, 1982.
- (25) Braslavsky, S. E.; Fron, E.; Rodriguez, H. B.; Román, E. S.; Scholes, G. D.; Schweitzer, G.; Valeur, B.; Wirz, J. *Photochem. Photobiol. Sci.* **2008**, 7, 1444.
- (26) Meer, B. W. V. D.; Coker, G.; Chen, S.-Y. S. *Resonance Energy Transfer: Theory and Data*; VCH: New York, 1994.
- (27) Lakowicz, J. R. *Principles of Fluorescence Spectroscopy*; Plenum Press: New York, 1983.
- (28) Cross, A. J.; Fleming, G. R. *Biophys. J.* **1984**, 46, 45–56.
- (29) McClain, W. M. *J. Chem. Phys.* **1972**, 57, 2264–2272.
- (30) Wagnière, G. J. *Chem. Phys.* **1982**, 76, 473–480.
- (31) Scholes, G. J. *Chem. Phys.* **2004**, 121, 10104–10110.
- (32) Gochanour, C. R.; Fayer, M. D. *J. Phys. Chem.* **1981**, 85, 1989.
- (33) Goodson, T. *Annu. Rev. Phys. Chem.* **2005**, 56, 581.
- (34) Andrews, D. L.; Blake, N. P. *J. Phys. A: Math. Gen.* **1989**, 22, 49–60.
- (35) Andrews, D. L.; Thirunamachandran, T. *J. Chem. Phys.* **1977**, 67, 5026.
- (36) Grage, M. M.-L.; Pullerits, T.; Ruseckas, A.; Theander, M.; Inganäs, O.; Sundström, V. *Chem. Phys. Lett.* **2001**, 339, 96.
- (37) Grage, M. M. L.; Zauschitsyn, Y.; Yartsev, A.; Chachivilis, M.; Sundström, V.; Pullerits, T. *Phys. Rev. B* **2003**, 67, 205207.
- (38) Grage, M. M.-L.; Wood, P. W.; Ruseckas, A.; Pullerits, T.; Mitchell, W.; Burn, P. L.; Samuel, I. D. W.; Sundström, V. *J. Chem. Phys.* **2003**, 118, 7644.
- (39) Westenhoff, S.; Daniel, C.; Friend, R. H.; Silva, C.; Sundström, V.; Yartsev, A. *J. Chem. Phys.* **2005**, 122, 094903.
- (40) Westenhoff, S.; Beenken, W. J. D.; Friend, R. H.; Greenham, N. C.; Yartsev, A.; Sundström, V. *Phys. Rev. Lett.* **2006**, 97, 166804.
- (41) Ruseckas, A.; Wood, P.; Samuel, I. D. W.; Webster, G. R.; Mitchell, W. J.; Burn, P. L.; Sundström, V. *Phys. Rev. B* **2005**, 72, 115214.
- (42) Chang, M. H.; Frampton, M. J.; Anderson, H. L.; Herz, L. M. *Phys. Rev. Lett.* **2007**, 98, 027402–1.
- (43) Bodunov, E. N.; Berberan-Santos, M. N.; Martinho, J. M. G. *Chem. Phys. Lett.* **2001**, 340, 137.
- (44) Hennebicq, E.; Pourtois, G.; Scholes, G. D.; Herz, L. M.; Russell, D. M.; Silva, C.; Setayesh, S.; Grimdale, A. C.; Müllen, K.; Brédas, J.-L.; Beljonne, D. *J. Am. Chem. Soc.* **2005**, 127, 4744.
- (45) Collini, E.; Scholes, G. D. *J. Phys. Chem. A* **2009**, 113, 4223.
- (46) Collini, E.; Scholes, G. D. *Science* **2009**, 323, 369.
- (47) Beljonne, D.; Pourtois, G.; Silva, C.; Hennbicq, E.; Herz, L. M.; Friend, R. H.; Scholes, G. D.; Setayesh, S.; Müllen, K.; Brédas, J. L. *Proc. Natl. Acad. Sci. U.S.A.* **2002**, 99, 10982–10987.
- (48) Wong, K. F.; Bagchi, B.; Rossky, P. J. *J. Phys. Chem. A* **2003**, 108, 5752.
- (49) Walla, P. J.; Linden, P. A.; Hsu, C.-P.; Scholes, G. D.; Fleming, G. R. *Proc. Natl. Acad. Sci. U.S.A.* **2000**, 97, 10808.
- (50) Czikkely, V.; Forsterling, H. D.; Khun, H. *Chem. Phys. Lett.* **1970**, 6, 207.
- (51) Czikkely, V.; Forsterling, H. D.; Khun, H. *Chem. Phys. Lett.* **1970**, 6, 11.
- (52) Beenken, W. J. D.; Pullerits, T. *J. Chem. Phys.* **2004**, 120, 2490.
- (53) Jordanides, X. J.; Scholes, G. D.; Fleming, G. R. *J. Phys. Chem. B* **2001**, 105, 1652.
- (54) Scholes, G. D.; Fleming, G. R. *J. Phys. Chem. B* **2000**, 104, 1854.
- (55) Nguyen, T.-Q.; Wu, J.; Tolbert, S. H.; Schwartz, B. J. *Adv. Mater.* **2001**, 13, 609.
- (56) Nguyen, T.-Q.; Wu, J.; Doan, V.; Schwartz, B. J.; Tolbert, S. H. *Science* **2000**, 288, 652.
- (57) Wiesenhofer, H.; Beljonne, D.; Scholes, G. D.; Hennebicq, E.; Brédas, J.-L.; Zojer, E. *Adv. Funct. Mater.* **2005**, 15, 155.
- (58) Ebihara, Y.; Vacha, M. *J. Phys. Chem. B* **2008**, 112, 12575.
- (59) Habuchi, S.; Onda, S.; Vacha, M. *Chem. Commun.* **2009**, 4868.
- (60) Sugimoto, T.; Ebihara, Y.; Ogino, K.; Vacha, M. *Chem. Phys. Chem.* **2007**, 8, 1623.
- (61) Sugimoto, T.; Habuchi, S.; Ogino, K.; Vacha, M. *J. Phys. Chem. B* **2009**, 113, 12220.
- (62) Schindler, F.; Lupton, J. M.; Feldmann, J.; Scherf, U. *Proc. Natl. Acad. Sci. U. S. A.* **2004**, 101, 14695.
- (63) Lin, H.; Tan, Y.; Zapadka, K.; Persson, G.; Thomsson, D.; Mirzov, O.; Larsson, P.-O.; Widengren, J.; Scheblykin, I. G. *Nano Lett.* **2009**, 9, 4456.
- (64) Weber, M. J. *Phys. Rev. B* **1971**, 4, 2932.
- (65) Burlakov, V. M.; Kawata, K.; Assender, H. E.; Briggs, G. A. D.; Ruseckas, A.; Samuel, I. D. W. *Phys. Rev. B* **2005**, 72, 075206.
- (66) Halls, J. J. M.; Pichler, K.; Friend, R. H.; Moratti, S. C.; Holmes, A. B. *Appl. Phys. Lett.* **1996**, 68, 3120.
- (67) Kroeze, J. E.; Savenije, T. J.; Vermeulen, M. J. W.; Warman, J. M. *J. Phys. Chem. B* **2003**, 107, 7696.
- (68) Lüer, L.; Egelhaaf, H.-J.; Oelkrug, D.; Cerullo, G.; Lanzani, G.; Huisman, B.-H.; de Leeuw, D. *Org. Electr.* **2004**, 5, 83.
- (69) Goh, C.; Scully, S. R.; McGehee, M. D. *J. Appl. Phys.* **2007**, 101, 114503–1.
- (70) Shaw, P. E.; Ruseckas, A.; Samuel, I. D. W. *Adv. Mater.* **2008**, 20, 3516–3520.
- (71) Wang, D.; Kopidakis, N.; Reese, M. O.; Gregg, B. A. *Chem. Mater.* **2008**, 20, 6307–6309.
- (72) Cook, S.; Liyuan, H.; Furube, A.; Katoh, R. *J. Phys. Chem. C* **2010**, 114, 10962.
- (73) Stoessel, M.; Wittmann, G.; Staudigel, J.; Steuber, F.; Blässing, J.; Roth, W.; Winnacker, A.; Inbasekaran, M.; Woo, E. P. *J. Appl. Phys.* **2008**, 87, 4467.
- (74) Kim, J.-S.; Friend, R. H.; Grizzi, I.; Burroughes, J. H. *Appl. Phys. Lett.* **2005**, 87, 023506.
- (75) Haugeneder, A.; Neges, M.; Kallinger, C.; Spirk, W.; Lemmer, U.; Feldmann, J. *Phys. Rev. B* **1999**, 59, 15346.
- (76) Markov, D. E.; Amsterdam, E.; Blom, P. W. M.; Sieval, A. B.; Hummelen, J. C. *J. Phys. Chem. A* **2005**, 109, 5266.
- (77) Markov, D. E.; Tanase, C.; Blom, P. W. M.; Wildeman, J. *Phys. Rev. B* **2005**, 72, 045217.
- (78) Scully, S. R.; McGehee, M. D. *J. Appl. Phys.* **2006**, 100, 034907.
- (79) Foster, S.; Finlayson, C. E.; Keivanidis, P. E.; Huang, Y.-S.; Hwang, I.; Friend, R. H.; Otten, M. B. J.; Lu, L.-P.; Schwartz, E.; Nolte, R. J. M.; Rowan, A. E. *Macromolecules* **2009**, 42, 2023.
- (80) Winfield, J. M.; Donley, C. L.; Kim, J.-S. *J. Appl. Phys.* **2007**, 102, 063505.
- (81) Godzik, K.; Jortner, J. *Chem. Phys. Lett.* **1979**, 63, 428.
- (82) Haan, S. W.; Zwanig, R. *J. Phys. Chem.* **1977**, 68, 1978.
- (83) Silbey, R. *Annu. Rev. Phys. Chem.* **1976**, 27, 203.
- (84) Gaab, K. M.; Bardeen, C. J. *J. Phys. Chem. A* **2004**, 108, 10801–10806.
- (85) Westenhoff, S.; Howard, I. A.; Friend, R. H. *Phys. Rev. Lett.* **2008**, 101, 016102.
- (86) Meskers, S. C. J.; Hübner, J.; Oestreich, M.; Bässler, H. *J. Phys. Chem. B* **2001**, 105, 9139.
- (87) Daniel, C.; Westenhoff, S.; Makereel, F.; Friend, R. H.; Beljonne, D.; Herz, L. M.; Silva, C. *J. Phys. Chem. C* **2007**, 111, 19111.
- (88) Ahn, T. S.; Wright, N.; Bardeen, C. J. *Chem. Phys. Lett.* **2007**, 446, 43.
- (89) Mollay, B.; Lemmer, U.; Kersting, R.; Kurz, H.; Göbel, E. O.; Bässler, H.; Kauffmann, H. F. *Phys. Rev. B* **1994**, 50, 10769.
- (90) Mizrov, O.; Cichos, F.; Borczykowski, C. v.; Scheblykin, I. G. *Chem. Phys. Lett.* **2004**, 386, 286.
- (91) Ruseckas, A.; Theander, M.; Valkunas, L.; Andersson, M. R.; Inganäs, O.; Sundström, V. *J. Lumin.* **1998**, 76&77, 474.
- (92) Huber, D. L. *Phys. Rev. B* **1979**, 20, 2307.
- (93) Athanasopoulos, S.; Hennebicq, E.; Beljonne, D.; Walker, A. B. *J. Phys. Chem. C* **2008**, 112, 11532.
- (94) McNeill, C. R.; Greenham, N. C. *Adv. Mater.* **2009**, 21, 3840.
- (95) Campbell, A. R.; Hodgkiss, J. M.; Westenhoff, S.; Howard, I. A.; Marsh, R. A.; McNeill, C. R.; Friend, R. H.; Greenham, N. C. *Nano Lett.* **2008**, 8, 3942.
- (96) Scully, S. R.; Armstrong, P. B.; Edder, C.; Frechet, J. M. J.; McGehee, M. D. *Adv. Mater.* **2007**, 19, 2961.
- (97) Dubin, F.; Melet, R.; Barisien, T.; Grousson, R.; Legrand, L.; Schott, M.; Voliotis, V. *Nat. Phys.* **2006**, 2, 32.
- (98) Lécuyer, R.; Berréhar, J.; Ganière, J. D.; Lapersonne-Meyer, C.; Lavallard, P.; Schott, M. *Phys. Rev. B* **2002**, 66, 125205.
- (99) Heun, S.; Mahrt, R. F.; Greiner, A.; Lemmer, U.; Bässler, H.; Halliday, D. A.; Bradley, D. D. C.; Burn, P. L.; Holmes, A. B. *J. Phys.: Condens. Matter* **1993**, 5, 247.
- (100) Rauscher, U.; Bässler, H. *Macromolecules* **1990**, 23, 398.
- (101) Heun, S.; Bässler, H.; Müller, U.; Müllen, K. *J. Phys. Chem.* **1994**, 98, 7355.
- (102) Romanovskii, Y. V.; Bässler, H. *J. Lumin.* **2005**, 113, 156–160.
- (103) Bogner, U.; Schatz, P.; Seel, R.; Maier, M. *Chem. Phys. Lett.* **1983**, 102, 267.
- (104) Offermans, T.; Meskers, S. C. J.; Janssen, R. A. J. *J. Chem. Phys.* **2003**, 119, 10924.
- (105) Marht, R.; Yang, J.-P.; Greiner, A.; Bässler, H. *Makromol. Chem., Rapid Commun.* **1990**, 11, 415.
- (106) Harrison, N. T.; Baigent, D. R.; Samuel, I. D. W.; Friend, R. H.; Grimdale, A. C.; Moratti, S. C.; Holmes, A. B. *Phys. Rev. B* **1996**, 53, 15815.

- (107) Bässler, H.; Schweitzer, B. *Acc. Chem. Res.* **1999**, *32*, 173–182.
- (108) Yu, Z.; Barbara, P. F. *J. Phys. Chem. B* **2004**, *108*, 11321.
- (109) Choi, S. H.; Kim, B.; Frisbie, C. D. *Science* **2008**, *329*, 1482.
- (110) Cho, M.; Yu, J.-Y.; Joo, T.; Nagasawa, Y.; Passino, S. A.; Fleming, G. R. *J. Phys. Chem.* **1996**, *100*, 11944.
- (111) Yang, X.; Dykstra, T. E.; Scholes, G. D. *Phys. Rev. B* **2005**, *71*, 045203.
- (112) Su, W. P.; Schrieffer, J. R.; Heeger, A. J. *Phys. Rev. Lett.* **1979**, *42*, 1698.
- (113) Heeger, A. J.; Kivelson, S.; Schrieffer, J. R.; Su, W. P. *Rev. Mod. Phys.* **1988**, *60*, 781.
- (114) Tretiak, S.; Saxena, A.; Martin, R. L.; Bishop, A. R. *Phys. Rev. Lett.* **2002**, *89*, 097402–1.
- (115) Beenken, W. J. D.; Pullerits, T. *J. Phys. Chem. B* **2004**, *108*, 6164.
- (116) Cornil, J.; Santos, D. A. d.; Crispin, X.; Silbey, R.; Brédas, J. L. *J. Am. Chem. Soc.* **1998**, *120*, 1289.
- (117) Beenken, W. J. D.; Dahlborn, M.; Kjellberg, P.; Pullerits, T. *J. Chem. Phys.* **2002**, *117*, 5810.
- (118) Beljonne, D.; Hennebicq, E.; Daniel, C.; Herz, L. M.; Silva, C.; Scholes, G. D.; Hoeben, F. J. M.; Jonkheijm, P.; Schenning, A. P. H. J.; Meskers, S. C. J.; Philips, R. T.; Friend, R. H.; Meijer, E. W. *J. Phys. Chem. B* **2005**, *109*, 10594.
- (119) Singh, J.; Bittner, E. R.; Beljonne, D.; Scholes, G. D. *J. Chem. Phys.* **2009**, *131*, 194905.
- (120) Dykstra, T. E.; Hennebicq, E.; Beljonne, D.; Gierschner, J.; Claudio, G.; Bittner, E. R.; Knoester, J.; Scholes, G. D. *J. Phys. Chem. B* **2009**, *113*, 656.
- (121) Chen, X.; Silbey, R. J. *J. Chem. Phys.* **2010**, *132*, 204503.
- (122) Fassioli, F.; Nazir, A.; Olaya-Catro, A. *J. Phys. Chem. Lett.* **2010**, *1*, 2139.
- (123) Daniel, C.; Strobel, T.; Dyakonov, V. *Phys. Rev. Lett.* **2009**, *103*, 036402.
- (124) Cornil, J.; Beljonne, D.; Shuai, Z.; Hagler, T. W.; Campbell, I.; Bradley, D. D. C.; Brédas, J. L.; Spangler, C. W.; Müllen, K. *Chem. Phys. Lett.* **1995**, *247*, 425.
- (125) Cornil, J.; Beljonne, D.; Heller, C. M.; Campbell, I. H.; Laurich, B. K.; Smith, D. L.; Bradley, D. D. C.; Müllen, K.; Brédas, J. L. *Chem. Phys. Lett.* **1997**, *278*, 139.
- (126) Karabunarliev, S.; Baumgarten, M.; Bittner, E. R.; Müllen, K. *J. Chem. Phys.* **2000**, *113*, 11372.
- (127) Karabunarliev, S.; Bittner, E. R.; Baumgarten, M. *J. Chem. Phys.* **2001**, *114*, 5863.
- (128) Zade, S. S.; Bendikov, M. *Chem. Eur. J.* **2007**, *13*, 3688.
- (129) Raos, G.; Famulari, A.; Marcon, V. *Chem. Phys. Lett.* **2003**, *379*, 364.
- (130) Beenken, W. J. D.; Lischka, H. *J. Chem. Phys.* **2005**, *123*, 144311.
- (131) Beljonne, D.; Shuai, Z.; Friend, R. H.; Brédas, J.-L. *J. Chem. Phys.* **1995**, *102*, 2042.
- (132) Gierschner, J.; Mack, H.-G.; Lüer, L.; Oelkrug, D. *J. Chem. Phys.* **2002**, *116*, 8596.
- (133) Heimel, G.; Daghofer, M.; Gierschner, J.; List, E. J. W.; Grimsdale, A. C.; Müllen, K.; Beljonne, D.; Brédas, J.-L.; Zojer, E. *J. Chem. Phys.* **2005**, *122*, 054501.
- (134) Darling, S. B.; Sternberg, M. *J. Phys. Chem. B* **2009**, *113*, 6215.
- (135) Grozema, F. C.; Duijnen, P. T. v.; Berlin, Y. A.; Ratner, M. A.; Siebbeles, L. D. A. *J. Phys. Chem. B* **2002**, *106*, 7791.
- (136) Beenken, W. J. D. *Chem. Phys.* **2008**, *349*, 250.
- (137) Liu, L. T.; Yaron, D.; Sluch, M. I.; Berg, M. A. *J. Phys. Chem. B* **2006**, *110*, 18844.
- (138) Liu, L. T.; Yaron, D.; Berg, M. A. *J. Phys. Chem. C* **2007**, *111*, 5770.
- (139) Franco, I.; Tretiak, S. *J. Am. Chem. Soc.* **2004**, *126*, 12130.
- (140) Barford, W.; Duffy, C. D. P. *Phys. Rev. B* **2006**, *74*, 075207.
- (141) Scholes, G. D.; Rumbles, G. In *Annual Review of Nano Research* 2; Cao, G., Brinker, C. J., Eds.; World Scientific Publishing: Hackensack, NJ, 2008; Vol. 2.